Masked Velocity Map Imaging: A One-Laser-Beam Doppler-Free Spectroscopic Technique†

Vasiliy Goncharov,‡ Nuradhika Herath,‡ Andrés Arregui,§ Luis Bañares,§ and Arthur G. Suits*,‡

Department of Chemistry, Wayne State University, Detroit, Michigan 48202, and Departamento de Quimica Fisica I, Facultad de Ciencias Quimicas, Universidad Complutense de Madrid, 28040 Madrid, Spain

Received: November 3, 2008; Revised Manuscript Received: December 10, 2008

A novel spectroscopic technique has been developed which makes it possible to record Doppler-free resonance-enhanced multiphoton ionization (REMPI) spectra with just one laser beam. The approach simply involves masking the outer side of the phosphor screen under velocity map imaging conditions so that only those species having no velocity component parallel to the laser beam propagation direction are detected. The benefits of this method are demonstrated in spectroscopic characterization of highly translationally and rotationally excited CO fragments resulted from the 230 nm photolysis of OCS and acetone, yielding substantially improved values of the rotational constants for the B state ($v'' = 0$) of the CO molecule. The resolving power and the state distribution analysis of reaction products are also demonstrated for room-temperature H atoms generated by dissociation of background hydrogen molecules and oxygen atom detected from the 225.6 nm photolysis of ozone.

I. Introduction

Since their first demonstration over 30 years ago, Doppler-free approaches[1−4] have become the methods of choice in virtually all applications where the very high spectral resolving power is needed. When combined with resonantly enhanced multiphoton ionization (REMPI), in addition to high-resolution, extraordinary sensitivity in detection can also be achieved. The intrinsic high sensitivity and high signal-to-noise ratio of REMPI become even more enhanced because all species in the detection volume are simultaneously in resonance. In a proof-of-principle experiment, Vrakking et al.[5] demonstrated that Doppler-free REMPI is an ultrasensitive probe (6.8×10^3 molecules/cm^3 for H_2) of quantum state distributions of reaction products. In recent years, Doppler-free or reduced-Doppler approaches have been applied to ion imaging studies with considerable success, and a number of variations of these techniques have emerged.[6−12]

In this paper we demonstrate another promising application for Doppler-free REMPI in velocity map imaging experiments. We propose a way to obtain Doppler-free REMPI spectra for spectroscopic studies and state distribution analysis of reaction products with just one laser beam. In all the above-mentioned experiments the Doppler-free spectra are achieved by exposing the molecules under study to a pair of counterpropagating laser beams. Taking into account the Doppler shifts caused by the velocity of the atoms or molecules, the frequencies of the photons appear symmetrically up-shifted and down-shifted in the molecule rest frame. When the pair of counterpropagating photons is absorbed the total two-photon energy becomes independent of the velocity, and hence the Doppler effect is canceled. There are a few experimental as well as fundamental complications in the two-photon Doppler-free scheme. Imperfect temporal or spatial overlap of two counterpropagating laser beams causes decrease in the detection efficiency.[6] Providing two laser beams instead of one can be time-consuming and a substantially more expensive endeavor especially in case of VUV lasers. On top of that, much higher laser power is needed to drive two-photon transitions compared to the one-photon ones. One laser beam signal as well as accidental one-photon resonances often deteriorate signal-to-noise ratios, but in principle, these can often be dealt with by changing laser beam polarizations.[7] Not all the transitions can be readily accessed and analyzed by two-photon methods due to the fundamental impediments in working out two-photon selection rules.

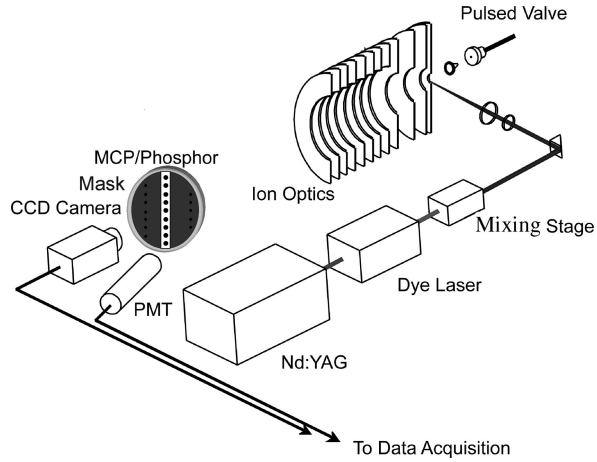

Figure 1. Experimental setup.

The approach presented here permits us to overcome all these complications by employing just one laser beam and restricting detection to only those species with zero velocity component along the laser propagation direction.

II. Experimental Section and Results

The schematic of the experimental setup utilized for this study is shown in Figure 1. The apparatus has been previously described[13] in great detail, except for one simple modification. A mask with a narrow vertical slit through the middle was placed

† Part of the "George C. Schatz Festschrift".

* To whom correspondence should be addressed. E-mail: asuits@chem.wayne.edu.

‡ Wayne State University.

§ Universidad Complutense de Madrid.

10.1021/jp809711n CCC: $40.75
Published on Web 01/26/2009

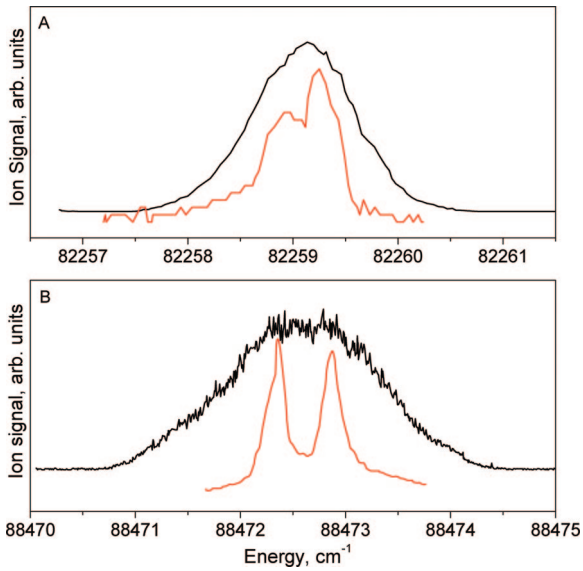

Figure 2. (A) Comparison between the masked 1 + 1′ Doppler-free REMPI (red spectrum) and conventional 1 + 1′ REMPI (black spectrum) of H atom via the H[2p^1] ^{2}P$_{1/2,3/2}$ ← H[1s^1] ^{2}S$_{1/2}$ transition at 82 258.921 cm^{-1} for $J' = {}^1/_2$ and 82 259.287 cm^{-1} for $J' = {}^3/_2$. The Doppler-free spectrum was collected with the outer side of the phosphor screen masked as depicted in Figure 1. The conventional (Doppler-broadened) spectrum was recorded with the unmasked detector. (B) Comparison between masked 2 + 1 Doppler-free REMPI (red trace) and conventional 2 + 1 REMPI (black trace) detection of O atom via the O[2s^{2}2p^{3}3p^1] ^{3}P$_{1,2}$ ← O[2s^{2}2p^4] ^{3}P$_1$ transition at 88 472.322 cm^{-1} for $J' = 1$ and 88 472.881 cm^{-1} for $J' = 2$.

on the outer side of a phosphor screen, in front of a photomultiplier tube (PMT). The width of the slit was varied depending on the UV laser line width and velocity of reaction products under study and was chosen to be roughly equal the portion of the Doppler profile corresponding to the laser line width to maximize sensitivity without sacrificing spectral resolution. For this purpose, the reaction products of interest were resonantly ionized by a UV laser at the center of the resonance and the mask was placed on the outer surface of the phosphor screen, before the PMT, with the slit size matching the Doppler profile observed in the middle of the phosphor screen (Figure 1). The 1 + 1′ ionization of H atoms via the [2p^1] ^{2}P$_{1/2,3/2}$ ← [1s^1] ^{2}S$_{1/2}$ REMPI transition was chosen to demonstrate the new technique. The H atoms were produced by a nude-type Bayard−Alpert gauge from background H_2 in the chamber. Tunable UV radiation with the wavelength around 121.6 nm was generated by frequency doubling of a dye laser output pumped by the second harmonic of a seeded Nd:YAG laser with subsequent tripling inside a VUV cell. Estimated VUV laser line width was around 0.25 cm^{-1}. Figure 2A shows a comparison between the 1 + 1′ masked REMPI (red spectrum) and unmasked 1 + 1′ REMPI (black spectrum) of H atoms via the H[2p^1] ^{2}P$_{1/2,3/2}$ ← H[1s^1] ^{2}S$_{1/2}$ transition at 82 258.921 cm^{-1} for $J' = {}^1/_2$ and 82 259.287 cm^{-1} for $J' = {}^3/_2$. Although the spacing between the lines is comparable to the VUV laser line width, two lines are clearly visible in the Doppler-free spectrum with the expected 1:2 line intensity ratio.

In a second experiment, the approach was demonstrated using REMPI of atomic oxygen produced by dissociation of ozone at 226 nm. The comparison between the masked 2 + 1 Doppler-free REMPI (red trace) and conventional 2 + 1 REMPI (black trace) detection of O atoms via the O[2s^{2}2p^{3}3p^1] ^{3}P$_{1,2}$ ← O[2s^{2}2p^4] ^{3}P$_1$ transition at 88 472.322 cm^{-1} for $J' = 1$ and at 88 472.881 cm^{-1} for $J' = 2$ is shown in Figure 2B. The 2 + 1

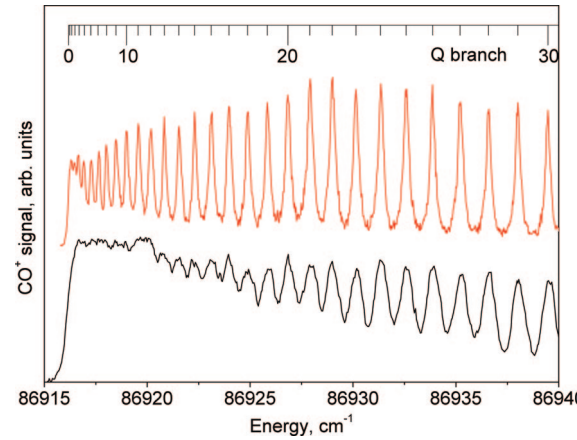

Figure 3. Portion of the 2 + 1 REMPI spectrum of the B $^1\Sigma^+(v' = 0)$ ← X $^1\Sigma^+(v'' = 0)$ transition of CO from acetone dissociation at 230 nm. The red trace is the masked Doppler-free spectrum, whereas the black trace is the conventional Doppler-broadened spectrum.

REMPI experiments were performed by sum-frequency mixing of the third harmonic of the seeded Nd:YAG laser and the fundamental output of the dye laser pumped by the second harmonic of the same Nd:YAG laser. Slightly narrower laser line width (about 0.15 cm^{-1}) and wider spacing between the lines permitted complete resolution of the O[2s^{2}2p^{3}3p^1] ^{3}P$_{1,2}$ ← O[2s^{2}2p^4] ^{3}P$_1$ atomic transitions. The O[2s^{2}2p^{3}3p^1] ^{3}P$_0$ ← O[2s^{2}2p^4] ^{3}P$_1$ transition at 88 473.038 cm^{-1} is forbidden according to the two-photon selection rules.[14] In the two cases presented so far, we resolve features in the excited state that are ordinarily summed over in detection. The ability to resolve these upper state features can be useful, for example, in detecting orbital polarization in photoproducts.[15]

In addition to the state distribution analysis of reaction products our Doppler-free REMPI technique can be applied in spectroscopic studies. For this purpose we recorded rotationally resolved B $^1\Sigma^+(v' = 0)$ ← X $^1\Sigma^+(v'' = 0)$ 2 + 1 REMPI spectra of CO produced in various degrees of rotational excitation. Acetone photolysis around 230 nm was utilized as a precursor for the moderately rotationally excited CO molecules ($J'' \leq 50$). Rotationally "hot" CO molecules with J'' ranging from around 35 to 80 were generated by the 230 nm photodissociation of OCS. Figures 3 and 4 illustrate a clear improvement in resolution when the masked Doppler-free REMPI is utilized to record rotationally resolved REMPI spectra of CO fragmented from acetone and OCS, respectively. The observed spectra were analyzed by fitting the rotational line positions of the B ← X Q-branch to the following expression:

$$\Delta E = T_{00} + (B'_0 - B''_0)J(J+1) - (D'_0 - D''_0)J^2(J+1)^2 + (H'_0 - H''_0)J^3(J+1)^3 \quad (1)$$

where T_{00} is the band origin; J is the rotational quantum number; B'_0, D'_0, H'_0 and B''_0, D''_0, H''_0 are rotational constants for the B $^1\Sigma^+(v' = 0)$ and X $^1\Sigma^+(v'' = 0)$ states of CO, respectively. The X $^1\Sigma^+(v'' = 0)$ state of CO has been extensively studied by microwave and infrared spectroscopy, and its molecular constants have been determined with exceptional degree of accuracy over a large data set of the rotational lines.[16] Therefore, very reliable molecular constants for the excited state can be obtained from the eq 1. Our fitting results along with previous measurements are illustrated in Table 1. Our data show noticeable improvement over previous measurements due to higher spectral resolution and broader data set of rotational levels. The deviations between the measured and fitted line

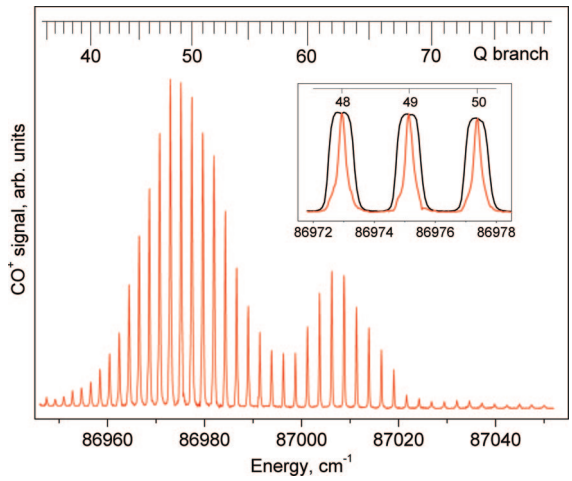

Figure 4. The 2 + 1 REMPI spectrum of the Q-branch of the B $^1\Sigma^+(v' = 0) \leftarrow$ X $^1\Sigma^+(v'' = 0)$ transition of CO from OCS dissociation at 230 nm acquired under the masked velocity mapping conditions. The inset shows comparison between the Doppler-free 2 + 1 REMPI spectrum shown in red and the conventional 2 + 1 REMPI spectrum shown in black.

TABLE 1: Comparison of Rotational Constants (in cm^{-1}) for the B $^1\Sigma^+(v' = 0)$ State of CO Obtained in This Study with the Reference Values

	this work	ref 18	ref 17	X $^1\Sigma^+(v'' = 0)$ const. (ref 16)
T_0	86 916.18[a]	86 916.18(3)	86 916.18[a]	
B_0	1.948 112(6)	1.948 186(72)	1.948 186[a]	1.922 528 96(8)
$D_0 \times 10^6$	6.6867(30)	6.784(21)	6.6355(12)	6.1203(10)
$H_0 \times 10^{12}$	−14.9(4)		−21.61(19)	5.48(2)
fwhm	≈0.25	≈0.6	≈0.8[b]	≈5 × 10^{-3}
data set size	$J' = 2-80$	$J' = 0-63$	$J' \sim 35-85$	$J'' \sim 0-94$

[a] Fixed during fitting procedure. [b] Estimated from our experiments under analogous conditions as in ref 17.

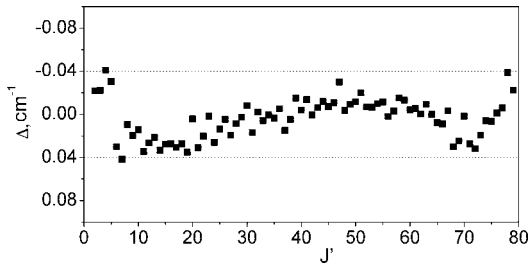

Figure 5. Difference between measured and fitted rotational line positions of the B $^1\Sigma^+(v' = 0)$ state of CO. In order to obtain a large data set of the CO line positions two "sources" of the rotationally hot CO were employed. For the low-J range of CO ($J'' = 0-50$) we used acetone dissociation, whereas high-J CO ($J'' = 35-80$) was produced by the OCS photodissociation.

positions are shown in Figure 5. These deviations are about 1 order of magnitude smaller than those derived from Doppler-broadened spectra of CO generated from the OCS photolysis[17] (fourth column in Table 1) and roughly 3 times smaller than in the VUV absorption and emission studies by Eidelsberg et al.[18] (third column in Table 1), where the rotational levels only up to $J' = 63$ were observed.

In some instances translational energy release of the reaction products varies substantially with the degree of rotational excitation. For example, high-J CO fragments from acetone photodissociation at 230 nm have translational energies around 0.3 eV, whereas low-J CO molecules show a clear bimodal distribution with translational energies of ≈0.05 and 0.3 eV (ref 11). In this case, in order to obtain accurate relative rotational state distributions, the inhomogeneous sampling of the velocity distribution by the slit placed on the detector must be taken into account. This effect leads to a bias in detection toward the ions with smaller kinetic energy release. To correct for the "slit effect," ion images of the entire ion cloud sliced through the slit were recorded for a wide range of J(CO) using the ion imaging acquisition software with a real-time ion counting method employing a center-of-mass calculation of each ion spot.[19] To recreate the full ion cloud signal from the "masked" signal, the ion counts for each pixel acquired with the masked detection were plotted as a function of the distance ρ between that pixel and the center of the image and multiplied by $\pi/(2 \arcsin\{W/2\rho\})$ if ρ was more than the half of the width of the slit, $W/2$. The images are assumed to be isotropic in this analysis. In case when acetone is chosen as CO precursor the image is isotropic irrespective of the laser polarization, but for anisotropic images the polarization can be adjusted to achieve isotropy. The ratios between the reconstructed and "masked" ion counts were obtained for several rotational levels of CO and used to extract unbiased relative rotational populations. This correction factor is important only when there are strongly varying populations of slow versus fast recoiling fragments. For the OCS results this is not the case, and no correction is necessary.

III. Discussion

Several research groups[20−22] have previously explored the idea of masked detection in imaging experiments. In the photodissociation study of CD_3I with 2 + 1 REMPI probe of the CD_3 fragments Janssen et al.[20] used a mask with a circular hole in the center to selectively detect only those methyl fragments traveling parallel to the photolysis laser polarization direction. Changing the polarization of the probe laser with respect to the photolysis laser polarization and monitoring the masked CD_3^+ signal then helped to extract the alignment moments $A_0^{(2)}$ and $A_0^{(4)}$. Mueller et al.[21] proposed a new technique, zero kinetic energy (ZKE) photofragment spectroscopy, where Rydberg-tagged fragments, after several hundred microsecond long flight times, were pulsed-field ionized at an imaging detector. Resulting fragments with zero kinetic energy were selectively monitored through a mask with a pinhole placed between a PMT and a phosphor screen. The authors demonstrated that this approach was especially suitable for the systems undergoing barrierless dissociation and can be employed in finding precise values of dissociation thresholds and in examining the transition state character.[21] Recently, Hopkins et al.[22] have pushed the resolution of H (Rydberg) atom photofragment translational spectroscopy to even higher limits using a slit-shaped mask to confine the detection only to those ions that have the same flight length.

Similar to above-mentioned techniques, our Doppler-free REMPI experiments rely on restricted detection of a particular group of ions, leading to a trade-off between the magnitude of signal and resolution. Although the line width of our lasers does not permit us to reveal this, the ion recoil energy and the velocity focusing conditions should also be considered as potential limits in achieving high spectral resolution. If the latter is satisfied then the fragments with the same velocity ionized at slightly different points will be focused on the same spot of the detector, facilitating the masked detection of only those ions with zero velocity component along the laser direction. We have recently demonstrated that in our "four-electrode" focusing lens setup, 0.17% limiting velocity resolution can be achieved, based on the ability to focus a large interaction volume to a single point.[19]

This means if the resolving power solely depended upon the focusing conditions then a spectral resolution on the order of 1 $\times 10^{-3}$ cm^{-1} could be readily achieved in B $^1\Sigma^+ \leftarrow$ X $^1\Sigma^+$ 2 + 1 REMPI spectra of CO. However, the ionization step can further compromise the resolution if the departing electron carries a substantial amount of energy. This is the case in the case of chosen REMPI detection scheme of CO, where the electron departs with the excess energy of more than 2 eV, resulting in 17 m/s of ion recoil velocity for the CO^+ ion. For the CO generated by the 230 nm photolysis of OCS this leads to 5 $\times 10^{-3}$ cm^{-1} spectral line width. Other factors such as molecular beam conditions and detector resolution will eventually need to be considered in the quest for the ultimate resolution with the proposed Doppler-fee approach.

IV. Conclusions

We have demonstrated a simple way to obtain Doppler-free REMPI spectra with just one laser beam in a velocity map imaging system. The new approach is particularly suitable for the spectroscopic studies and state distribution analysis of reaction products with large translational energies.

Acknowledgment. A.A. acknowledges financial support for a short stay at Wayne State University through the FPI program of the Spanish Ministry of Education and Science. This work was supported by the Director, Office of Science, Office of Basic Energy Science, Division of Chemical Science, Geoscience and Bioscience, of the U.S. Department of Energy under contract no. DE-FG02-04ER15593.

References and Notes

(1) Vasilenko, L. S.; Chebotayev, V. P.; Shishaev, A. V. *Zh. Eksp. Teor. Fiz., Pis'ma Red.* **1970**, *12*, 161.
(2) Biraben, F.; Cagnac, F.; Grynberg, G. *Phys. Rev. Lett.* **1974**, *32*, 643.
(3) Levenson, M. D.; Bloembergen, N. *Phys. Rev. Lett.* **1974**, *32*, 645.
(4) Hansch, T. W.; Harvey, K.; Meisel, G.; Schawlow, A. L. *Opt. Commun.* **1974**, *11*, 50.
(5) Vrakking, M. J. J.; Bracker, A. S.; Suzuki, T.; Lee, Y. T. *Rev. Sci. Instrum.* **1993**, *64*, 645.
(6) Pomerantz, A. E.; Zare, R. N. *Chem. Phys. Lett.* **2003**, *370*, 515.
(7) Riedel, J.; Dziarzhytski, S.; Kuczmann, A.; Renth, F.; Temps, F. *Chem. Phys. Lett.* **2005**, *414*, 473.
(8) Huang, C. S.; Li, W.; Kim, M. H.; Suits, A. G. *J. Chem. Phys.* **2006**, *125*, 121101.
(9) Huang, C. S.; Lahankar, S. A.; Kim, M. H.; Zhang, B. L.; Suits, A. G. *Phys. Chem. Chem. Phys.* **2006**, *8*, 4652.
(10) Goldberg, N. T.; Koszinowski, K.; Pomerantz, A. E.; Zare, R. N. *Chem. Phys. Lett.* **2007**, *433*, 439.
(11) Goncharov, V.; Herath, N.; Suits, A. G. *J. Phys. Chem. A* **2008**, *112*, 9423.
(12) Radenovic, D. C.; van Roij, A. J. A.; Wu, S. M.; Ter Meulen, J. J.; Parker, D. H.; van der Loo, M. P. J.; Janssen, L. M. C.; Groenenboom, G. C. *Mol. Phys.* **2008**, *106*, 557.
(13) Townsend, D.; Minitti, M. P.; Suits, A. G. *Rev. Sci. Instrum.* **2003**, *74*, 2530.
(14) Bonin, K. D.; McIlrath, T. J. *J. Opt. Soc. Am. B* **1984**, *1*, 52.
(15) Suits, A. G.; Vasyutinskii, O. S. *Chem. Rev.* **2008**, *108*, 3706.
(16) Guelachvili, G.; Devilleneuve, D.; Farrenq, R.; Urban, W.; Verges, J. *J. Mol. Spectrosc.* **1983**, *98*, 64.
(17) Rijs, A. M.; Backus, E. H. G.; de Lange, C. A.; Janssen, M. H. M.; Westwood, N. P. C.; Wang, K. S.; McKoy, V. *J. Chem. Phys.* **2002**, *116*, 2776.
(18) Eidelsberg, M.; Roncin, J. Y.; Lefloch, A.; Launay, F.; Letzelter, C.; Rostas, J. *J. Mol. Spectrosc.* **1987**, *121*, 309.
(19) Li, W.; Chambreau, S. D.; Lahankar, S. A.; Suits, A. G. *Rev. Sci. Instrum.* **2005**, *76*, 063106.
(20) Janssen, M. H. M.; Parker, D. H.; Sitz, G. O.; Stolte, S.; Chandler, D. W. *J. Phys. Chem.* **1991**, *95*, 8007.
(21) Mueller, J. A.; Rogers, S. A.; Houston, P. L. *J. Phys. Chem. A* **1998**, *102*, 9666.
(22) Hopkins, W. S.; Loock, H. P.; Cronin, B.; Nix, M. G. D.; Devine, A. L.; Dixon, R. N.; Ashfold, M. N. R. *J. Chem. Phys.* **2007**, *127*, 064301.

JP809711N